Single-Step Formation of Degradable Intracellular Biomolecule Microreactors

Marijke Dierendonck,[†,⊥] Stefaan De Koker,[†,‡,⊥] Riet De Rycke,[§] Pieter Bogaert,[§] Johan Grooten,[‡] Chris Vervaet,[†] Jean Paul Remon,[†] and Bruno G. De Geest[†,*]

[†]Laboratory of Pharmaceutical Technology, Department of Pharmaceutics, Ghent University, Ghent, Belgium, [‡]Laboratory of Molecular Immunology, Department of Biomedical Molecular Biology, Ghent University, Zwijnaarde, Belgium, and [§]Department of Molecular Biomedical Research, VIB, Zwijnaarde, Belgium. [⊥]These authors contributed equally to this work.

ABSTRACT Here we present a single-step all-aqueous approach to encapsulate biomolecules such as enzymes and proteins into stable microreactors. Key in this method is the use of spray-drying of the biomolecules of interest in combination with oppositely charged polyelectrolytes and mannitol as the sacrificial template. Remarkably, upon spray-drying in the presence of polyelectrolyte, mannitol crystallization is suppressed and the obtained amorphous mannitol offers enhanced preservation of the biomolecules' activity. Moreover, the use of mannitol allows the formation of nanopores within the microparticles upon rehydration of the microparticles in aqueous medium and subsequent dissolution of the mannitol. The oppositely charged polyelectrolytes provide a polymeric framework which stabilizes the microparticles upon rehydration. The versatility of this approach is demonstrated using horseradish peroxidase as the model enzyme and ovalbumin as the model antigen.

KEYWORDS: drug delivery · microparticles · polyelectrolytes · vaccines · dendritic cells

Microparticulate encapsulation strategies have gained increased interest for the encapsulation of biomolecules for drug delivery or to serve as a microreactor. We hypothesize that fully hydrated microparticles should exhibit superior properties for applications such as intracellular protein delivery and as an enzyme microreactor where one desires to separate the enzyme physically from the surrounding medium. Our hypothesis is supported by the fact that fully hydrated microparticles allow in- and outward diffusion of water as well as reactants and reaction products. Moreover, microparticles with additionally a porous interconnected structure should allow an even faster and more efficient intraparticle processing as the presence of pores along with a higher surface to volume ratio, which allows efficient access, especially of macromolecular reactants such as proteins which would encounter serious diffusion limitation to enter densely structured microparticles.[1]

A wide spectrum of synthetic methods to produce porous microparticles has been described in the literature and was recently reviewed by Gokmen *et al.*[2] Generally, the synthesis involves the use of organic solvents as well as reactive chemistries such as radical polymerization or condensation reactions. In our research group, we are developing polyelectrolyte-based microparticles using merely water-based solutions of oppositely charged polyelectrolytes that self-assemble through electrostatic interaction. An intriguing class of polyelectrolyte-based microparticles are polyelectrolyte multilayered[3] microcapsules[4,5] These microparticles are made by sequential deposition of oppositely charged species onto a charged template followed by the decomposition of this template. By depositing typically 2−5 polyelectrolyte bilayers onto microparticles with sizes typically between 500 nm and 10 μm, hollow capsules can be designed. A striking feature of these microparticles is that they are perm-selective, meaning that low molecular weight species such as solvents, ions, and metabolites can freely diffuse in- and outward.[6] However, high molecular weight species such as proteins remain entrapped within the capsules. In our group, we are particularly interested in developing microparticulate vaccines that specifically target their payload to antigen-presenting cells, such as dendritic cells,[7−12] the work horses of our immune system. Both our group[8,10] and the Caruso group[13,14] reported that such multilayered capsules, based on degradable polymers, were efficiently taken up by dendritic cells both *in vitro* and *in vivo* and are excellent inducers of T-cell responses. Several other groups have described the use of such capsules as an enzyme microreactor comprising enzymes that are stably

* Address correspondence to br.degeest@ugent.be.

Received for review March 8, 2011 and accepted July 18, 2011.

Published online August 25, 2011
10.1021/nn200901g

encapsulated either inside the hollow void of the capsules or into the shell.[15−18]

Despite numerous advantages, the major drawback of LbL capsules is their multistep fabrication involving several centrifugation−redispersion steps per deposited polyelectrolyte layer. Moreover, in a typical LbL procedure, polyelectrolytes are deposited from solutions containing approximately a 100-fold excess of polyelectrolyte while the non-adsorbed polyelectrolytes are usually wasted. Therefore, we envisioned to develop simplified procedures to produce polyelectrolyte microparticles while maintaining as much as possible their versatile properties. In a previous study, we reported on the use of spray-drying to produce porous polyelectrolyte microparticles by co-spray-drying oppositely charged polyelectrolytes with calcium carbonate nanoparticles as the sacrificial component followed by extraction of the calcium carbonate nanoparticles with an EDTA solution.[19] This two-step procedure allowed the efficient incorporation of ovalbumin as a model antigen into porous microparticles that were efficiently taken up by dendritic cells, envisioning application in microparticulate vaccine delivery.

In this article, we demonstrate that by co-spray-drying polyelectrolytes with mannitol—a water-soluble well-established pharmaceutical excipient—nanoporous polyelectrolyte microparticles can be produced that allow protein encapsulation with nearly 100% efficiency with excellent preservation of biological activity. Moreover, a dry powder formulation is obtained which offers additional benefits for long-time storage (essential for vaccine applications), only requiring reconstitution in aqueous medium at the time of use. Spray-drying is widely used in the pharmaceutical industry and is commonly used to convert water-soluble species into a water-soluble dry powder. By contrast, the novelty of our method involves a nanodispersion of polyelectrolyte complexes with proteins that are subsequently formulated through spray-drying into spherical microparticles that remain stable upon rehydration in aqueous medium. Key in this work is the use of a fully biocompatible (*i.e.*, mannitol) water-soluble sacrificial component that readily dissolves upon redispersion of the spray-dried microparticles in water. In this way, additional steps to remove and purification steps to dissolve organic (*e.g.*, polystyrene or melamine formaldehyde latexes) or inorganic (*e.g.*, calcium carbonate or silica particles) core templates are avoided.

Using horseradish peroxidase (HRP) as the model enzyme, we demonstrate that enzymatic activity is retained within the microparticles, indicating the potential of the system as an enzymatic microreactor. Furthermore, in an *in vitro* model for vaccine delivery using ovalbumin (OVA) as the model antigen, we demonstrated that encapsulated OVA is readily processed by intracellular lysosomal proteases of dendritic cells, and subsequently, the CD8 epitope of OVA is presented on the cell surface as an MHCI complex. This process is termed cross-presentation, meaning that extracellular antigen becomes internalized and presented to $CD8^+$ T-cells, which is crucial to induce cellular immune responses to combat intracellular viral pathogens as well as cancer. In this sense, the microparticles act as intracellular protein microreactors.

RESULTS AND DISCUSSION

An aqueous dispersion (1% w/w) was prepared by mixing mannitol, dextran sulfate (DS), and ovalbumin under stirring followed by dropwise addition of poly-L-arginine (P_LARG) to allow electrostatic complexation between DS, OVA, and P_LARG. The ratio (w/w) of mannitol to OVA, DS, and P_LARG was chosen to be 40:1:4:5, respectively, which is based on our previous experience with hollow LbL capsules and porous polyelectrolyte microspheres based on calcium carbonate as the sacrificial template. Subsequently, the mixture was spray-dried using a lab-scale Buchi B290 spray-drier and collected as a dry powder (Figure 1A1,A2). Upon addition of water, the mannitol readily dissolves and stable microparticles consisting of a polyelectrolyte framework encapsulating the co-spray-dried protein remains (Figure 1B1,B2). Laser diffraction (Figure 1D) measurements on these particles show a mean diameter of 7 μm.

To allow visualization by fluorescence microscopy, green fluorescent OVA-Alexa488 was used and the confocal images in Figure 1C1−C3 confirm that the green fluorescent OVA-Alexa488 is retained within the porous microspheres rather than being released into the surrounding aqueous medium. To assess the spatial distribution of polyelectrolytes and mannitol, a batch of microspheres was produced with both the OVA (Alexa488) and the poly-L-arginine fluorescently labeled. Confocal microscopy images of the microspheres upon rehydration (Figure 1E) demonstrate that the OVA is homogeneously distributed throughout the whole microsphere volume while the poly-L-arginine shows a slightly higher concentration near the microsphere surface. Quantification of the encapsulation efficiency was done by resuspending the particles in phosphate buffered saline (PBS; pH = 7.4 and 150 mM NaCl). Subsequently, the microspheres were centrifuged and the amount of OVA in the supernatant was measured. The encapsulation efficiency is defined as the amount of protein that is retained within the microparticles after resuspending relative to the amount of protein in the dry microparticles. After resuspension in PBS, an encapsulation efficiency of 99 ± 1% was calculated. This encapsulation efficiency is remarkably higher than previously reported, not only for OVA encapsulation within hollow LbL capsules (50% encapsulation efficiency for calcium

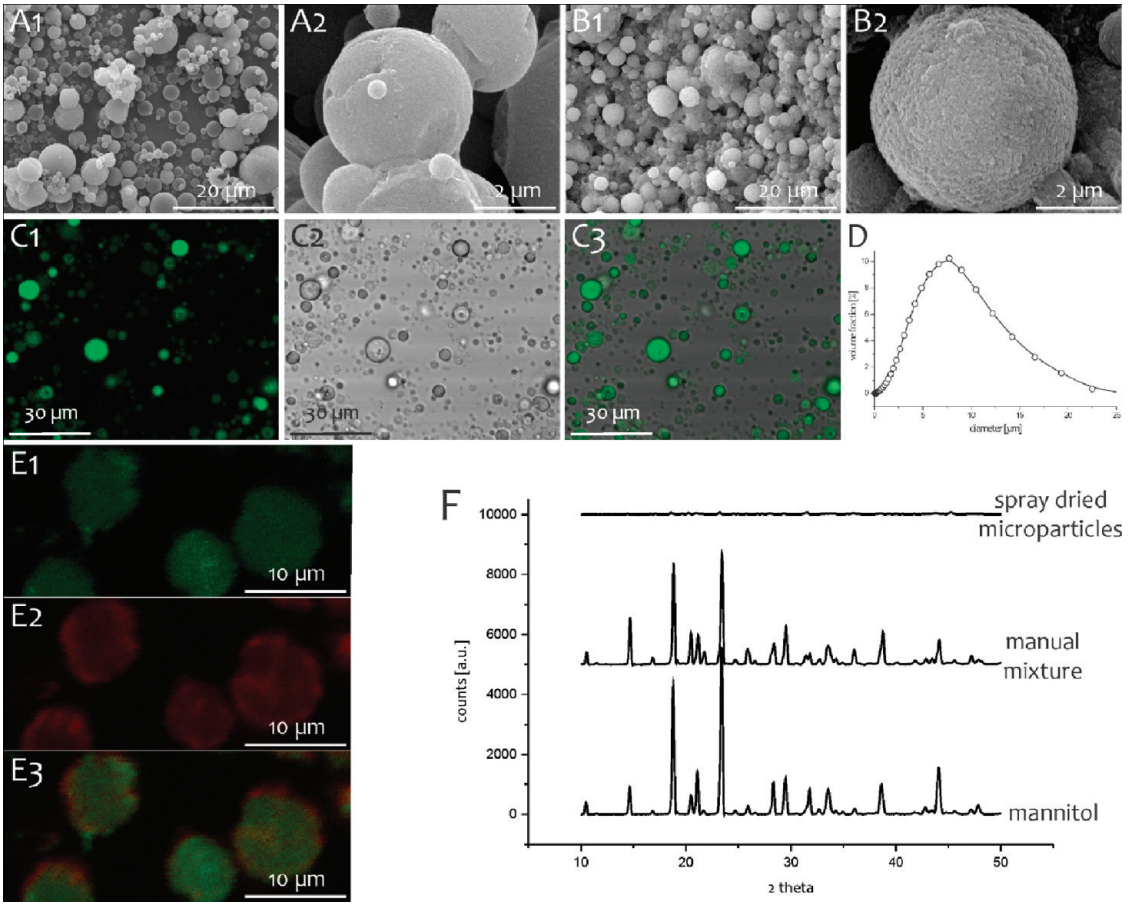

Figure 1. Physicochemical characterization of spray-dried polyelectrolyte microspheres. (A,B) Scanning electron microscopy images of spray-dried polyelectrolyte microspheres (A) before and (B) after removal of mannitol. (C) Confocal microscopy images of the spray-dried polyelectrolyte microspheres dispersed in water. Alexa488 (green fluorescence)-conjugated ovalbumin was encapsulated as model antigen. (D) Size distribution of the spray-dried polyelectrolyte microspheres obtained by laser diffraction. (E) Confocal microscopy images of double-labeled microspheres containing Alexa488-conjugated ovalbumin (E1), rhodamine isothiocyanate-conjugated poly-L-arginine (E2). (E3) Overlay of the green and red fluorescence channel. (F) X-ray powder diffractograms of pure mannitol, a mannitol/polyelectrolyte physical mixture, and spray-dried polyelectrolyte microspheres.

carbonate template capsules which offer the highest encapsulation efficiency of all types of LbL capsules)[8,10] but also within porous antigen-loaded degradable polyelectrolyte microspheres with calcium carbonate as the sacrificial template (85% encapsulation efficiency).[19] In order to compare our spray-dried microspheres with the "gold standard" in drug delivery, we encapsulated OVA in poly(DL-lactide-*co*-glycolide (PLGA) microspheres using a general procedure reported by Lynn and Langer.[20] Figure S3 in the Supporting Information shows microscopy images and size distribution of these microspheres that have a mean diameter of 0.5 μm as measured by laser diffraction. The encapsulation efficiency was determined by measuring the concentration of fluorescently labeled (Alexa488) OVA in the supernatant after centrifugation of the particles and found to be 63 $\pm$ 15%, which is again substantially lower than in the case of the spray-dried polyelectrolyte microspheres. Moreover, the OVA/polymer ratio is 1:100 in the case of PLGA while it is 1:10 in the case of the spray-dried polyelectrolyte microspheres, indicating that much fewer polymers are required to keep the OVA stably encapsulated. Moreover, the synthesis of PLGA microspheres requires the use of organic solvents, which involves safety as well as environmental risks.

Further physicochemical characterization of the microspheres was done by X-ray powder diffraction (XRPD; Figure 1F). The crystallographic state of mannitol after spray-drying is important because amorphous mannitol could provide enhanced protection of encapsulated proteins against denaturation. Several papers have indeed reported on the role of proteins in retaining mannitol in amorphous form after spray-drying.[21,22] However, in those cases, amorphous mannitol could only be obtained at very high protein concentrations, which were prone to denaturation upon spray-drying. Figure 1F shows the XRPD diffractograms of crude mannitol, physically dry mixed mannitol, DS, P_LARG and OVA, and finally the spray-dried microparticles. Crude mannitol is crystalline with characteristic peaks at 10.6 and 14.7°, and the XRPD spectrum of the physically dry mixture of

mannitol, DS, P_LARG, and OVA showed crystallinity similar to that of pure mannitol, indicating that merely mixing of the substances did not lead to any change in their crystallographic state. By contrast, the diffractograms of the spray-dried particles exhibit a dramatic reduction of crystallinity, indicating the formation of amorphous mannitol. Note that OVA spray-dried with mannitol without polyelectrolytes also yielded crystalline mannitol and that spray-dried mannitol with polyelectrolytes also yielded amorphous mannitol in the absence of OVA (data not shown).

For applications in drug delivery as well as to serve as a microreactor for enzymatic processing, the preservation of the biological activity of the encapsulated protein within the polyelectrolyte framework is of paramount importance. Therefore, we encapsulated an enzyme, horseradish peroxidase (HRP), instead of OVA and compared the enzymatic catalytic activity (*i.e.*, rate of substrate conversion) by the free HRP enzyme in solution to the rates of conversion yielded by the aqueous mannitol/DS/HRP/P_LARG dispersion and by the HRP-loaded spray-dried microparticles. This was performed by following the increase in UV−vis absorbance at 403 nm due to the conversion of the substrate ABTS (2,2′- azinobis(3-ethylbenzothiazoline-6-sulfonic acid)diammonium salt) by HRP:

$$H_2O_2 + 2ABTS + 2H^+ \xrightarrow{HRP} 2\ \text{radical cation}^{\lambda = 403nm} + 2H_2O$$

From the slope of the obtained kinetic curves, the enzymatic catalytic activity (Figure 2A) was derived. When the rate of conversion of ABTS by free HRP free solution is equal to 100%, an activity of 87 ± 3% for the physical mixture and 84 ± 5% for the spray-dried microparticles is calculated. This shows that, upon mixing, a 13 ± 3% drop in enzymatic activity occurs which is likely due to electrostatic interaction with the DS/P_LARG polyelectrolyte complexes.[15] As HRP has an isoelectric point of ~8.8, it is positively charged at neutral pH and is likely to undergo complexation with DS. Most strikingly, the spray-drying process itself only induces a further activity decrease of merely 3%.

As a control, we also measured the enzymatic activity of HRP spray-dried with DS/P_LARG but without mannitol and the enzymatic activity of HRP spray-dried with mannitol but without the polyelectrolytes DS/P_LARG. Without mannitol, bumped dense microparticles were obtained (see Figure S1 in the Supporting Information for SEM images), which could only be recovered at very low yields, most likely due to electrostatic interaction with the glass wall of the spray-drying cylinder. The enzymatic activity of the encapsulated HRP was measured to be 50 ± 8%, which is significantly lower than in the case of mannitol/DS/HRP/P_LARG microparticles.

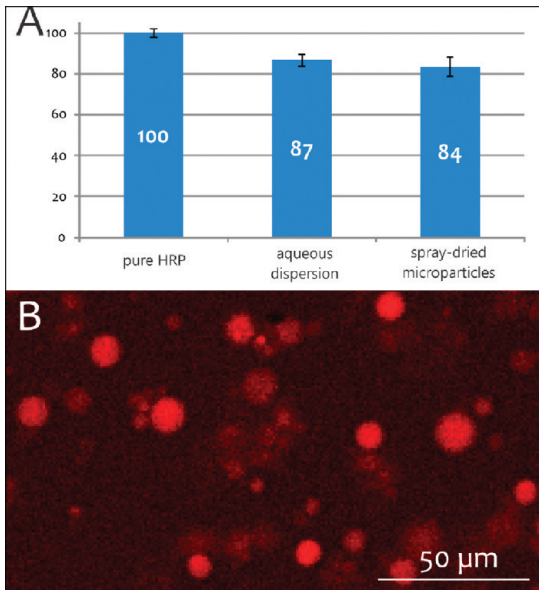

Figure 2. (A) Quantification of the relative enzymatic activity by conversion of 2,2′-azinobis(3-ethylbenzothiazoline-6-sulfonic acid)diammonium salt (ABTS) by free horseradish peroxidase (HRP) in solution, an aqueous dispersion of mannitol, polyelectrolyte and HRP, and spray-dried microparticles after resuspension in phosphate buffered saline (PBS). (B) Confocal microscopy image showing the conversion of Amplex Red to resorufin (red fluorescence) within the spray-dried microspheres after addition of H_2O_2.

Microparticles consisting solely of HRP and mannitol, thus without polyelectrolytes, were also obtained as a perfectly spherical-shaped powder (see Supporting Information for SEM images). They dissolve readily upon addition of water, yielding a solution rather than a microparticle suspension obtained in the case of spray-dried mannitol/DS/HRP/P_LARG microparticles. Moreover, the enzymatic activity of the encapsulated HRP was measured to be 61 ± 12%, which is again significantly lower than in the case of mannitol/DS/HRP/P_LARG microparticles. Taking into account that XRPD measurements on the mannitol/HRP microparticles (without polyelectrolytes) show the mannitol to be in a crystalline state (see Supporting Information Figure S2) while the presence of polyelectrolytes yields amorphous mannitol, we hypothesize that the presence of amorphous mannitol strongly augments the preservation of the enzymatic activity of encapsulated HRP.

Thus the encapsulation approach demonstrated in this work allows a much higher preservation (*i.e.*, 84 ± 5%) of HRP activity compared to common LbL polyelectrolyte capsules or amphiphilic vesicles where typically a reduction of 50−85% of enzymatic activity upon encapsulation is observed.[15,18,23] Moreover, these other encapsulation strategies suffer from far lower encapsulation efficiencies compared to our spray-drying approach. To demonstrate that enzymatic reaction occurs inside the spray-dried microparticles,

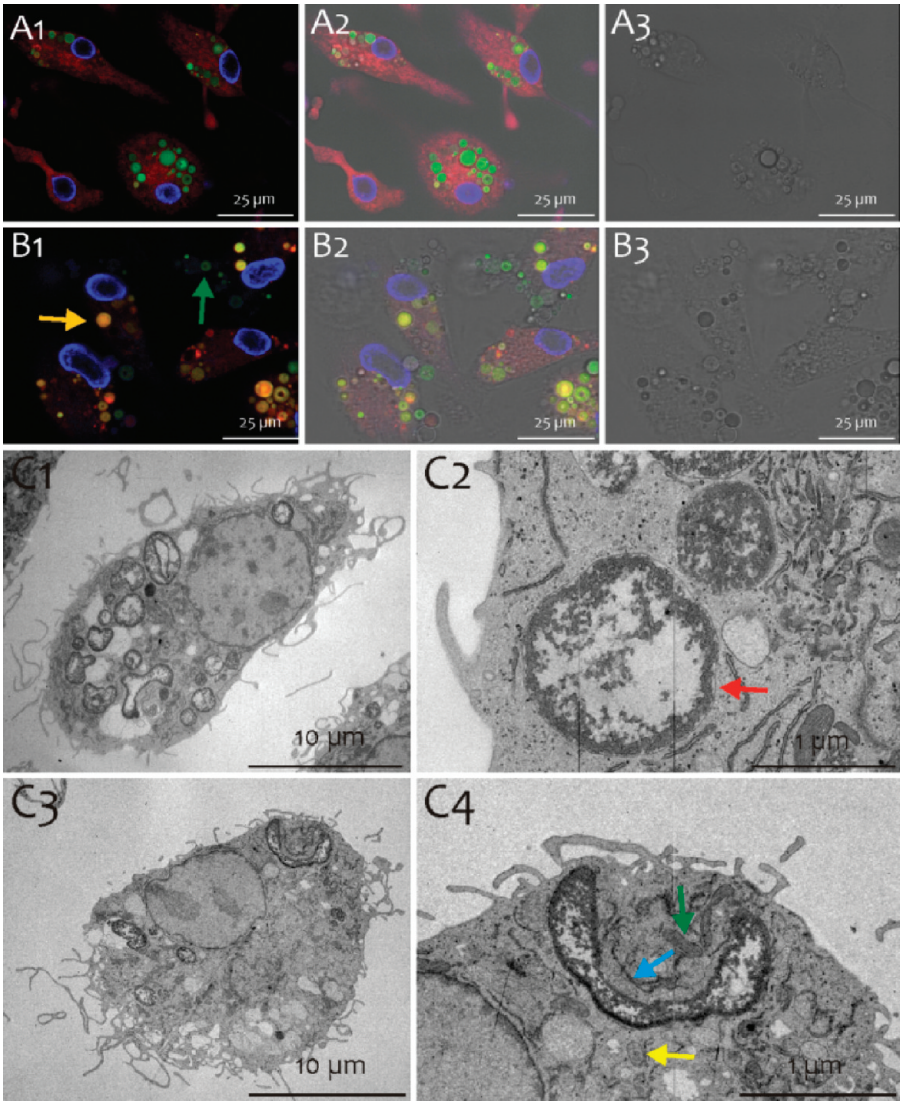

Figure 3. Assessment of cellular uptake of the spray-dried polyelectrolyte microspheres by dendritic cells. (A,B) Confocal microscopy images of dendritic cells incubated with spray-dried polyelectrolyte microspheres loaded with Alexa488-conjugated ovalbumin (green fluorescence). In row A, the cellular cytoplasm was stained with CellTracker Red (red fluorescence). In row B, the intracellular acidic vesicles (phagosomes, endosomes, lysosomes) were stained with LysoTracker Red (red fluorescene). In both cases, the cell nuclei were stained with Hoechst (blue fluorescence). Column 1 shows the overlay between the blue, green, and red channels, column 2 shows the overlay between the blue, green, red, and DIC (differential interference contrast) channels, and column 3 shows the DIC channel. (C) Transmission electron microscopy images of spray-dried polyelectrolyte microspheres internalized by dendritic cells after (C1,C2) 4 h and (C3,C4) 24 h of incubation.

we used Amplex Red as the fluorogenic substrate instead of ABTS. In the presence of H_2O_2, Amplex Red is converted by HRP to resorufin, which is strongly fluorescent. Figure 2B shows a confocal microscopy image after addition of Amplex Red and H_2O_2 to a mannitol/DS/HRP/P_LARG microparticle suspension. The fluorescent microspheres indicate that reaction takes place inside the microspheres[24] followed by diffusion of the dye, coloring the medium.

In the next series of experiments, we investigated the interaction of the polyelectrolyte microspheres with dendritic cells (DCs), which are the primary target cell population for vaccine delivery. In this work, we used DCs derived from bone marrow of mice. Figure 3A,B shows confocal microscopy images of DCs incubated with spray-dried microparticles loaded with OVA-Alexa488 (green fluorescence). In Figure 3A, the cellular cytoplasm was stained red fluorescent with CellTracker Red, and in Figure 3B, the intracellular acidic vesicles (phagosomes, endosomes, lysosomes) were stained red fluorescent with LysoTracker Red. From the overlay between the fluorescence image and the DIC (differential interference contrast) channel in Figure 3A2, it is evident that the polyelectrolyte microparticles became internalized. In Figure 3B1, co-localization—expressed as a yellow/orange signal—between the green fluorescence of the polyelectrolyte microparticles and the red fluorescence of the

intracellular vesicles is observed. For clarity of presentation, we have marked in Figure 3B1 an internalized polyelectrolyte microparticle with an orange arrow and marked a non-internalized polyelectrolyte microparticle with a green arrow. These data indicate that upon internalization the polyelectrolyte microparticles end up in intracellular acidic vesicles, which is common for most types of microparticles so far reported in the literature.[8,25] More detail on the intracellular behavior of the internalized microparticles was obtained by imaging ultrathin sections of epoxy-embedded DCs by transmission electron microscopy (TEM). Figure 3C shows TEM images of DCs incubated for 4 h (Figure 3C1,C2) and 24 h (Figure 3C3,C4).

Following uptake, the particles were surrounded by a membrane (red arrow, Figure 3C2), which indicates that the particles end up in phagolysosomal compartments following uptake, as was also previously described for hollow LbL capsules. These data are also in accordance with the observed colocalization with LysoTracker Red, as shown in Figure 3B1. The TEM images in Figure 3C3,C4 clearly demonstrate that after 1 day incubation the polyelectrolyte microparticles become deformed, and the zoomed image in Figure 3C4 shows the recruitment of different intracellular organelles such as ER (blue arrow), mitochondria (green arrow), and lysosomes (yellow arrow) toward the deformed polyelectrolyte microparticle. These TEM data indicate an active intracellular processing of the internalized polyelectrolyte microparticles and puts them en route toward potential application in vaccine delivery.

Finally, we aimed to assess whether the encapsulated OVA is still available for processing upon internalization by DCs and, if so, whether the peptide fragments become cross-presented *via* a peptide–MHC class I complex. Following endocytosis, soluble exogenous antigens are generally cleaved by lysosomal proteases and presented *via* a peptide–MHC class II complex to CD4 T-cells. DCs also harbor the capacity to present exogenous antigens *via* MHCI, a feature called cross-presentation that is necessary to prime CD8 cytotoxic T-cells capable of killing virally infected cells. However, cross-presentation of soluble antigens occurs extremely inefficiently but is dramatically augmented when the antigen is in a particulate form, as was found for several types of microparticulate antigen carriers.[8,26,27] To address whether this important feature also holds true for the spray-dried polyelectrolyte microspheres, we incubated DCs with equivalent amounts of soluble OVA and OVA encapsulated in either hollow LbL capsules, PLGA microspheres, or spray-dried polyelectrolyte microspheres. After a 48 h incubation period, DCs were stained with the 25-D1.16 mAb which specifically recognizes the SIINFEKL OVA-CD8+ epitope complexed to MHC class I H-2Kb molecules.[28]

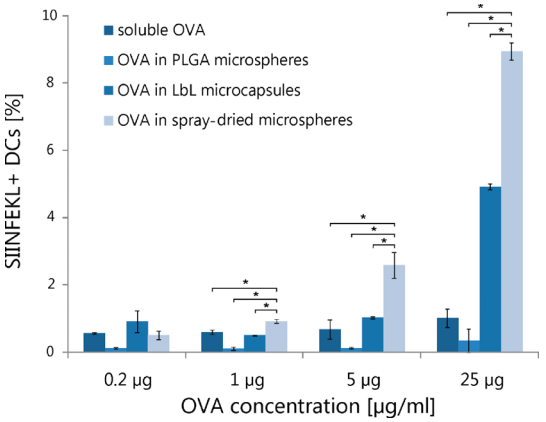

Figure 4. Cross-presentation of the SIINFEKL OVA-CD8 peptide measured by FACS analysis on 25-D1.16 mAb stained DCs that were incubated with soluble OVA, OVA encapsulated in PLGA microspheres, OVA encapsulated in hollow LbL capsules, and OVA encapsulated in spray-dried polyelectrolyte microspheres. Experiments were run in triplicate. The polymers used for fabricating the LbL capsules were the same as those used for the spray-dried polyelectrolyte microspheres (*i.e.*, dextran sulfate and poly-L-arginine). An asterix "*" indicates the statistically significant groups.

As shown in Figure 4, a dose-dependent increase in cross-presentation of encapsulated OVA was observed when compared to the soluble antigen. Spray-dried particles were significantly more potent than PLGA and hollow LbL capsules in stimulating antigen cross-presentation. This is most likely due to the fact that the spray-dried polyelectrolyte microspheres carry more antigen per particle compared to hollow LbL capsules and PLGA microspheres, thus delivering more antigen when a DC internalizes a particle. Moreover, the spray-dried polyelectrolyte microspheres allow readily processing of the encapsulated antigen due to their fully hydrated structure, which is not the case for PLGA microspheres which gradually release their payload through surface-erosion-based degradation and therefore are incapable of inducing antigen cross-presentation within the experimental time frame of 48 h.

In conclusion, we have demonstrated in this paper a one-step all-aqueous approach to encapsulate proteins into polyelectrolyte microspheres. The role of the polyelectrolytes is two-fold. The first is to form stable microspheres upon redispersion of the spray-dried powder in water. Second, the polyelectrolyte framework suppresses the mannitol crystallization—used as additional excipient for spray-drying—which is shown to be beneficial for both the bioactivity of encapsulated proteins as well as for the process yield. Furthermore, these data indicate that the spray-drying process does not dramatically hamper intracellular proteases to enter the polyelectrolyte matrix and to subsequently process the antigen into peptide fragments allowing their presentation onto the DC

surface. The observed cross-presentation paves the road to further develop this technology as a vaccine delivery platform for insidious viral pathogens as well as cancer.

METHODS

Materials. Mannitol was obtained from Cargill. Dextran sulfate (DS; $M_w \sim 9-20$ kDa), poly-L-arginine (P_LARG; $M_w > 70$ kDa), poly(DL-lactide-*co*-glycolide) (PLGA; 50:50, $M_w \sim 40-75$ kDa), poly(vinyl alcohol) (PVA; 80% hydrolyzed, $M_w \sim 9-10$ kDa), ovalbumin (OVA), horseradish peroxidase (HRP), 2,2′-azinobis(3-ethylbenzothiazoline-6-sulfonic acid)diammonium salt (ABTS), and Ampliflu red (Amplex Red) were obtained from Sigma-Aldrich. Phosphate buffered saline (PBS), OVA-Alexa488, CellTracker Red, and LysoTracker Red were obtained from Invitrogen. H_2O_2 was obtained from Fagron. All water used in the experiments was of Milli-Q grade.

Synthesis of (Porous) Microspheres. Mannitol, DS, OVA, and P_LARG were mixed in water in a 40:4:1:5 ratio at a total solid concentration of 1%. In detail, 200 mg of mannitol, 20 mg of DS, and 5 mg of OVA were dissolved in 20 mL of water. Subsequently, 25 mg of P_LARG was dissolved in 5 mL of water and added dropwise to the stirring mannitol/DS/OVA dispersion. This was carried out analogously for the HRP microspheres. Spray-drying of these mixtures was performed in a lab-scale Bucchi B290 spray-dryer. The mixture was fed to a two fluid nozzle (diameter 0.7 mm) at the top of the spray-dryer. In addition, the spray-dryer operated in cocurrent air flow at drying air temperature of 130 °C. Fluorescent microparticles were prepared using a mixture of OVA with Alexa488 (green fluorescence)-conjugated ovalbumin in a 50:1 ratio.

Synthesis of PLGA Microspheres. OVA was encapsulated in PLGA microspheres according to a general procedure reported by Lynn and Langer.[20] An aqueous OVA solution (200 μL; 10 mg/mL) was emulsified by 10 s sonication in 4 mL of dichloromethane containing 200 mg of PLGA. This primary emulsion was then emulsified in 50 mL of an aqueous 1% PVA solution using a Silverson high shear homogenizer for 30 s at maximum power. Subsequently, the obtained secondary emulsion was diluted with 100 mL of an aqeuous 0.5% PVA solution and stirred for 3 h under ambient conditions to allow evaporation of dichloromethane. Finally, the hardened PLGA microspheres were collected by centrifugation (10 min at 4000*g*) and washed three times with deionized water. The encapsulation efficiency of OVA was determined by encapsulating Alexa488-conjugated OVA instead of blank OVA and subsequently measuring the OVA-Alexa488 concentration in the supernatant using a Perkin-Elmer Envision multilabel plate reader.

Particle Characterization. Confocal microscopy images were recorded on a Leica SP5 AOBS confocal microscope. Scanning electron microscopy images were recorded on a quanta FEG FEI 200 apparatus. Samples were dried on a silicon wafer and sputtered with a thin layer of palladium/gold. Transmission electron microscopy images of ultrathin microtomed sections were recorded on a JEOL 1010 electron microscope. Laser diffraction was performed on a Malvern Mastersizer equipped with a 300 RF objective. The ζ-potential measurements were performed on a Malvern Nanosizer ZS. X-ray powder diffractograms were performed on a PANalytical X'Pert PRO X-ray diffractometer (Siemens). XRPD patterns were obtained with Cu Kα radiation (45 kV $\times$ 40 mA; λ = 1.5406 A) at a scanning speed of 25° (2θ)/min and step size of 0.03° (2θ). Measurements were done in the reflection mode in the 2θ range of 5−40°. Analysis of the diffractograms was done by visual inspection. The encapsulation efficiency was determined by resuspending a known amount of OVA-Alexa488-loaded microparticles (thus containing a known amount of protein (protein conc$^{\text{dry microparticles}}$) in phosphate buffered saline followed by centrifugation and measuring the OVA-Alexa488 concentration (protein conc$^{\text{supernatant}}$) in the supernatant using a Perkin-Elmer Envision multilabel plate reader. The encapsulation efficiency is then calculated as follows:

$$\text{encapsulation efficiency} = 100 \times \frac{\text{proteinconc}^{\text{dry microparticles}} - \text{protein conc}^{\text{supernatant}}}{\text{protein conc}^{\text{dry microparticles}}}$$

Determination of Enzymatic Activity. Enzymatic activity of encapsulated HRP was monitored by measuring the absorbance at 405 nm with a Perkin-Elmer Envision multilabel plate reader. In detail, 0.1 mL of ABTS solution (0.01 mg/mL) and 0.1 mL of a HRP solution (0.00025 mg/mL) or 0.1 mL of resuspended spray-dried microparticles (0.0125 mg/mL in 0.1 M phosphate buffer) or a aqueous dispersion of mannitol, DS, P_LARG, and HRP (0.0125 mg/mL in 0.1 M phosphate buffer) was mixed in the wells of a 96-well plate. Then 0.1 mL of a H_2O_2 solution (0.03%) was added. The absorbance was measured every 20 s at 405 nm, and the reaction was allowed to proceed for 5 min. Each reaction was carried out in six-fold. Visualization by confocal microscopy was performed using Amplex Red as a fluorogenic substrate. A 50 μL drop of microparticle suspension (5 mg/mL) was put on a microscope coverslip followed by the addition of 2 μL of 0.05 mg/mL Amplex Red and 3 μL of H_2O_2 (20 mM). Confocal images were recorded using a Leica SP5 AOBS confocal microscope by excitation with the 561 nm laser line and detection at 580 nm.

DC Uptake Assessment. Female C57BL/6 mice were purchased from Janvier and housed in a specified pathogen-free facility in microisolator units. Dendritic cells were generated using a modified Inaba protocol. Two to six month old C57BL/6 mice were sacrificed, and bone marrow was flushed from their femurs and tibias. After lysis of red blood cells with ACK lysis buffer (BioWhittaker), granulocytes and B-cells were depleted using Gr-1 (Pharmingen) and B220 (Pharmingen) antibodies, respectively, and low-toxicity rabbit complement (Cedarlane Laboratories Ltd.). Cells were seeded at a density of 2×10^5 cells/mL in 175 cm^2 Falcon tubes (Becton Dickinson) in DC medium (RPMI 1640 medium containing 5% LPS-free FCS, 1% penicillin/streptomycin, 1% L-glutamine, and 50 μM β-mercaptoethanol) containing 10 ng/mL of IL-4 and 10 ng/mL of GM-CSF (both from Peprotech). After 2 days and again after 4 days of culture, the non-adherent cells were centrifuged, resuspended in fresh medium, and replated to the same falcons. On the sixth day, non-adherent cells were removed and fresh medium containing 10 ng/mL of GM-CSF and 5 ng/mL of IL-4 was added.

On day 8 of culture, non-adherent cells were harvested and seeded in Lab-Tek (Nunc, Thermo Scientific) 8-chambered cover glasses. The spray-dried microparticles were suspended in PBS at a concentration corresponding of 0.5 mg/mL of OVA, and 10 μL of this suspension was added to the DCs. After 2 h incubation, the cells were fixed in an aqueous 4% formaldehyde solution overnight. Subsequently, the cells were washed three times with PBS and stained with Hoechst 33258 (2 μg/mL). For the assessment of the intracellular localization of the porous microspheres, cells were not fixed with formaldehyde, and the cellular cytoplasm and acidic vesicles were stained by CellTracker Red (1 μg/mL) and LysoTracker Red (1 μg/mL), respectively, and directly visualized by confocal microscopy.

Determination of MHCI Presentation. To assess the capacity of spray-dried particles to enhance antigen presentation of encapsulated antigen, bone-marrow-derived dendritic cells were isolated as described above and incubated with a dilution series of either soluble ovalbumin or the equivalent amount of ovalbumin encapsulated in spray-dried particles. Forty-eight hours later, cells were stained with anti-CD11c-APC (BD Biosciences) and 25D1.16-PE (Ebioscience), which specifically recognizes the ovalbumin-derived peptide SIINFEKL presented by MHCI at the cell surface. Samples were analyzed by flow cytometry (Becton Dickinson, LSRII). Specificity of the antibody

staining was verified by pulsing DC with PBS, which showed a negligible SIINFEKL detection of 0.23%, while DC directly pulsed with SIINFEKL showed a detection of 91%. Statistical analysis was performed using an one-way ANOVA with Bonferroni post-hoc test ($p < 0.05$ = significant).

Acknowledgment. M.D. thanks Ghent University for a Ph.D. scholarship (BOF-GOA). S.D.K. thanks Ghent University for a BOF scholarship. B.D.G. thanks the FWO for a postdoctoral scholarship and Ghent University (BOF-GOA) and FWO for funding. P.B. acknowledges Ghent University for support through a Methusalem (BOF09/01M00709) grant. Dr. Els Mehuys is acknowledged for help with the statistical interpretation.

Supporting Information Available: Additional experimental microscopy and X-ray powder diffraction data. This material is available free of charge *via* the Internet at http://pubs.acs.org.

REFERENCES AND NOTES

1. Jain, S.; Yap, W. T.; Irvine, D. J. Synthesis of Protein-Loaded Hydrogel Particles in an Aqueous Two-Phase System for Coincident Antigen and CpG Oligonucleotide Delivery to Antigen- Presenting Cells. *Biomacromolecules* **2005**, *6*, 2590–2600.
2. Gokmen, M. T., Du Prez, F. E. Porous Polymer Particles—A Comprehensive Guide to Synthesis, Characterization, Functionalization and Applications. *Prog. Polym. Sci.*, in press.
3. Decher, G. Fuzzy Nanoassemblies: Toward Layered Polymeric Multicomposites. *Science* **1997**, *277*, 1232–1237.
4. Caruso, F.; Caruso, R. A.; Mohwald, H. Nanoengineering of Inorganic and Hybrid Hollow Spheres by Colloidal Templating. *Science* **1998**, *282*, 1111–1114.
5. Donath, E.; Sukhorukov, G. B.; Caruso, F.; Davis, S. A.; Mohwald, H. Novel Hollow Polymer Shells by Colloid-Templated Assembly of Polyelectrolytes. *Angew. Chem., Int. Ed.* **1998**, *37*, 2202–2205.
6. Sukhorukov, G. B.; Brumen, M.; Donath, E.; Mohwald, H. Hollow Polyelectrolyte Shells: Exclusion of Polymers and Donnan Equilibrium. *J. Phys. Chem. B* **1999**, *103*, 6434–6440.
7. De Geest, B. G.; Vandenbroucke, R. E.; Guenther, A. M.; Sukhorukov, G. B.; Hennink, W. E.; Sanders, N. N.; Demeester, J.; De Smedt, S. C. Intracellularly Degradable Polyelectrolyte Microcapsules. *Adv. Mater.* **2006**, *18*, 1005.
8. De Koker, S.; De Geest, B. G.; Singh, S. K.; De Rycke, R.; Naessens, T.; Van Kooyk, Y.; Demeester, J.; De Smedt, S. C.; Grooten, J. Polyelectrolyte Microcapsules as Antigen Delivery Vehicles to Dendritic Cells: Uptake, Processing, and Cross-Presentation of Encapsulated Antigens. *Angew. Chem., Int. Ed.* **2009**, *48*, 8485–8489.
9. De Koker, S.; Lambrecht, B. N.; Willart, M. A. M.; Van Kooyk, Y.; Grooten, J.; Vervaet, C.; Remon, J. P.; De Geest, B. G. Designing Polymeric Particles for Antigen Delivery. *Chem. Soc. Rev.* **2011**, *40*, 320–339.
10. De Koker, S.; Naessens, T.; De Geest, B. G.; Bogaert, P.; Demeester, J.; De Smedt, S. C.; Grooten, J. Biodegradable Polyelectrolyte Microcapsules: Antigen Delivery Tools with Th17 Skewing Activity after Pulmonary Delivery. *J. Immunol.* **2010**, *184*, 203–211.
11. De Cock, L. J.; Lenoir, J.; Vermeersch, V.; De Koker, S.; Skirtach, A. G.; Dubruel, P.; Adriaens, E.; Vervaet, C.; Remon, J. P.; De Geest, B. G. Polyelectrolyte Induced *In Vivo* Mucosal Irritation Is Dramatically Reduced upon Complexation. *Biomaterials* **2011**, *32*, 1967–1977.
12. De Geest, B. G.; De Koker, S.; Gonnissen, Y.; De Cock, L. J.; Grooten, J.; Remon, J. P.; Vervaet, C. A Single Step Process for the Synthesis of Antigen Laden Thermosensitive Microparticles. *Soft Matter* **2010**, *6*, 305–310.
13. De Rose, R.; Zelikin, A. N.; Johnston, A. P. R.; Sexton, A.; Chong, S. F.; Cortez, C.; Mulholland, W.; Caruso, F.; Kent, S. J. Binding, Internalization, and Antigen Presentation of Vaccine-Loaded Nanoengineered Capsules in Blood. *Adv. Mater.* **2008**, *20*, 4698–4703.
14. Sexton, A.; Whitney, P. G.; Chong, S. F.; Zelikin, A. N.; Johnston, A. P. R.; De Rose, R.; Brooks, A. G.; Caruso, F.; Kent, S. J. A Protective Vaccine Delivery System for *In Vivo* T Cell Stimulation Using Nanoengineered Polymer Hydrogel Capsules. *ACS Nano* **2009**, *3*, 3391–3400.
15. Balabushevich, N. G.; Sukhorukov, G. B.; Larionova, N. I. Polyelectrolyte Multilayer Microspheres as Carriers for Bienzyme System: Preparation and Characterization. *Macromol. Rapid Commun.* **2005**, *26*, 1168–1172.
16. Kreft, O.; Prevot, M.; Mohwald, H.; Sukhorukov, G. B. Shell-in-Shell Microcapsules: A Novel Tool for Integrated, Spatially Confined Enzymatic Reactions. *Angew. Chem., Int. Ed.* **2007**, *46*, 5605–5608.
17. Wang, Y. J.; Caruso, F. Nanoporous Protein Particles through Templating Mesoporous Silica Spheres. *Adv. Mater.* **2006**, *18*, 795–800.
18. Stein, E. W.; Volodkin, D. V.; McShane, M. J.; Sukhorukov, G. B. Real-Time Assessment of Spatial and Temporal Coupled Catalysis within Polyelectrolyte Microcapsules Containing Coimmobilized Glucose Oxidase and Peroxidase. *Biomacromolecules* **2006**, *7*, 710–719.
19. Dierendonck, M.; De Koker, S.; Cuvelier, C.; Grooten, J.; Vervaet, C.; Remon, J. P.; De Geest, B. G. Facile Two Step Synthesis of Porous Antigen Loaded Degradable Polyelectrolyte Microspheres. *Angew. Chem., Int. Ed.* **2010**, *49*, 8620–8624.
20. Lynn, D. M.; Amiji, M. M.; Langer, R. pH-Responsive Polymer Microspheres: Rapid Release of Encapsulated Material within the Range of Intracellular pH. *Angew. Chem., Int. Ed.* **2001**, *40*, 1707–1710.
21. Hulse, W. L.; Forbes, R. T.; Bonner, M. C.; Getrost, M. Influence of Protein on Mannitol Polymorphic Form Produced during Co-spray Drying. *Int. J. Pharm.* **2009**, *382*, 67–72.
22. Andya, J. D.; Maa, Y. F.; Costantino, H. R.; Nguyen, P. A.; Dasovich, N.; Sweeney, T. D.; Hsu, C. C.; Shire, S. J. The Effect of Formulation Excipients on Protein Stability and Aerosol Performance of Spray-Dried Powders of a Recombinant Humanized Anti-IgE Monoclonal Antibody. *Pharm. Res.* **1999**, *16*, 350–358.
23. Vriezema, D. M.; Garcia, P. M. L.; Oltra, N. S.; Hatzakis, N. S.; Kuiper, S. M.; Nolte, R. J. M.; Rowan, A. E.; van Hest, J. C. M. Positional Assembly of Enzymes in Polymersome Nanoreactors for Cascade Reactions. *Angew. Chem., Int. Ed.* **2007**, *46*, 7378–7382.
24. Yashchenok, A. M.; Delcea, M.; Videnova, K.; Jares-Erijman, E. A.; Jovin, T. M.; Konrad, M.; Mohwald, H.; Skirtach, A. G. Enzyme Reaction in the Pores of $CaCO_3$ Particles upon Ultrasound Disruption of Attached Substrate-Filled Liposomes. *Angew. Chem., Int. Ed.* **2010**, *49*, 8116–8120.
25. Javier, A. M.; Kreft, O.; Semmling, M.; Kempter, S.; Skirtach, A. G.; Bruns, O. T.; del Pino, P.; Bedard, M. F.; Raedler, J.; Kaes, J.; *et al.* Uptake of Colloidal Polyelectrolyte-Coated Particles and Polyelectrolyte Multilayer Capsules by Living Cells. *Adv. Mater.* **2008**, *20*, 4281–4287.
26. Moon, J. J.; Suh, H.; Bershteyn, A.; Stephan, M. T.; Liu, H.; Huang, B.; Sohail, M.; Luo, S.; Ho Um, S.; Khant, H.; *et al.* Interbilayer-Crosslinked Multilamellar Vesicles as Synthetic Vaccines for Potent Humoral and Cellular Immune Responses. *Nat. Mater.* **2011**, *10*, 243–251.
27. Broaders, K. E.; Cohen, J. A.; Beaudette, T. T.; Bachelder, E. M.; Frechet, J. M. J. Acetalated Dextran Is a Chemically and Biologically Tunable Material for Particulate Immunotherapy. *Proc. Natl. Acad. Sci. U.S.A.* **2009**, *106*, 5497–5502.
28. Palankar, R.; Skirtach, A. G.; Kreft, O.; Bedard, M.; Garstka, M.; Gould, K.; Mohwald, H.; Sukhorukov, G. B.; Winterhalter, M.; Springer, S. Controlled Intracellular Release of Peptides from Microcapsules Enhances Antigen Presentation on MHC Class I Molecules. *Small* **2009**, *5*, 2168–2176.